Convolutional Deep Belief Network Based Expert System for Automated Fault Diagnosis in Hydro Electrical Power Systems

[1]Husam Alowaidi, [2]Prashant G C, [3]Gopalakrishnan T, [4]Sundar Rajan M, [5]Padmaja S M and [6]Anjali Devi S
[1]Department of Information Technology, College of Science, University of Warith Al-Anbiyaa, Karbala, Iraq.
[2]Department of Computer Science, Texas Tech University, Lubbock, USA.
[3]Department of Information Technology, Manipal Institute of Technology Bengaluru,
Manipal Academy of Higher Education, Manipal, Karnataka, India.
[4]Faculty of Electrical and Computer Engineering, Arbaminch Institute of Technology, Arbaminch University, Ethiopia.
[5]Department of Electrical and Electronics Engineering, Shri Vishnu Engineering College for Women, Bhimavaram, Andhra Pradesh, India.
[6]Department of Computer Science and Engineering, Koneru Lakshmaiah Education Foundation, Vaddeswaram, Guntur, Andhra Pradesh, India.
[1]husam@uowa.edu.iq, [2]prashantgc2000@gmail.com, [3]gopalakrishnan.ct@gmail.com, [4]msundarrajan84@gmail.com, [5]padmaja_vvr@yahoo.com, [6]swarnaanjalidevi@gmail.com

Correspondence should be addressed to Gopalakrishnan T : gopalakrishnan.ct@gmail.com.

Article Info
Journal of Machine and Computing (http://anapub.co.ke/journals/jmc/jmc.html)
Doi: https://doi.org/10.53759/7669/jmc202404031
Received 10 March 2023; Revised from 30 October 2023; Accepted 12 January 2024.
Available online 05 April 2024.

Abstract – The paper developed an approach for fault diagnosis in Hydro-Electrical Power Systems (HEPS). Using a Renewable Energy System (RES), HEPS has performed a significant part in contributing to addressing the evolving energy demands of the present. Several electro-mechanical elements that collectively comprise the Hydro-Electric (HE) system are susceptible to corrosion from routine usage and unplanned occurrences. Administration and servicing systems that are successful in implementing and achieving these goals are those that regularly track and predict failures. Detect models applied in the past included those that were primarily reactive or reliant on human involvement to identify and analyse abnormalities. The significant multiple variables intricacies that impact successful fault detection are disregarded by these frameworks. The research presented here proposes a Convolutional Deep Belief Network (CDBN) driven Deep Learning (DL) model for successful fault and failure detection in such power systems that address these problems. Applying sample data collected from two Chinese power plants, the proposed framework has been assessed compared to other practical DL algorithms. Different metrics have been employed to determine the effectiveness of the simulations, namely Accuracy, Precision, Recall, and F1-score. These outcomes indicated that the CDBN is capable of predicting unexpected failures. Graphic representations demonstrating control used to measure turbine blade load, vibration level, and generator heat for assessing the replicas.

Keywords – Hydro-Electrical Power Systems, Convolutional Deep Belief Network, Renewable Energy System, Smart Grid, Deep Learning, Accuracy, Precision, Recall, and F1-score.

I. INTRODUCTION

In the industry of Hydro-Electric Power Systems (HEPS), it has become of the highest priority to maintain an operational system that is both cost-effective and reliable. Understanding the essential function that these systems perform in facilitating the production of Renewable Energy (RE), it is significant to recognise that they tend to be highly susceptible to unsafe mechanical and environmental factors, which may contribute to the malfunction of equipment [1]. In addition to the reality that these types of malfunctions have brought about a major disruption in the distribution of electrical energy, they additionally resulted in significant expenses for repairing and restoration.

The traditional Fault Diagnosis Methods (FDM) that have been employed by HEPS, consisting of physical testing and basic threshold-based tracking systems, are the main emphasis and core of the current study [2]. A great deal of these frameworks are responsive instead of proactive because they frequently find these anomalies after a malfunction occurred previously. When they have to deal with the test, they tend to be reactive. The threat of major harm and operational downtime is now more significant due to an interruption in monitoring operations. It has become challenging to predict and mitigate the effects of possible failures in HEPS, and the wide range of failure modes—which encompasses both hard and soft failures—only renders problems better [3].

Current existing solutions that were employed for the purpose of fault diagnosis in the domain of HEPS have already included various Machine Learning (ML) and data analysis techniques. However, these methods all come with certain limitations; such learning models probably may not fully capture the complex and dynamic interactions within the system or else such models may involve extensive manual feature engineering [4]. Deep Learning (DL) models that are employed for these problems are used to offer a more advanced solution, which process by automatically learning features from data. Even such models, when applied in HEPS, are faced with particular challenges that include the need for large datasets, computational resources, and expertise in model tuning [5]. This research is trying to deal with those problems by designing and assessing a Convolutional Deep Belief Network (CDBN)-Based Expert System. The purpose of this study aims to tackle those problems. This method has invented a technique that utilises the benefits of Convolutional Neural Networks (CNN) and Deep Belief Networks (DBN) in order to enhance fault detection and classification. This strategy is capable of helping to address a few of the draw backs of traditional approaches by presenting a FMD that is more precise, effective, and proactive in HEPS.

The design, implementation, and assessment of a Convolutional Deep Belief Network-based Expert System (CDBN-ES) for the objective of Automated Fault Diagnosis (AFD) in HEPS is the main goal of the project. A model that facilitates the utilisation of CDBN-ES to recognise and classify faults in hydroelectric power stations was developed as the outcome of the findings from this study. For the intention of learning the model, input was collected from two generators, GR04 and GR17, which had been chosen from hydroelectric power plants situated in China. The present work develops a Fault Detection Model (FDM) that detects two primary failure modes: hard failures, triggered by severe operational stresses or mechanical motion obstacles, and soft failures, which create progressively throughout uninterrupted operation according to normal or relatively demanding conditions. The recommended FDM examines data collected by sensors on vibration, heat, and pressure parameters to precisely imitate the generator's performance and anticipate possible malfunctions, allowing the switch from reactive to proactive maintenance scheduling. To assess the effectiveness of these models, we utilized performance metrics such as Accuracy, Precision, Recall, and F1-score. The performance of the FDM model was presented through control for stress on turbine blades, vibration frequency, and generator temperature, which demonstrated the models' ability to highlight deviations that are indicative of potential issues. The comparative analysis indicated the CDBN model's superior performance for fault detection, thereby emerging as the most effective approach for predictive maintenance strategies in HEPS.

The work is presented as follows: **Section 2** presents the literature review, **Section 3** presents the methodology, **Section 4** presents the experiment analysis, and **Section 5** presents the conclusion.

II. LITERATURE REVIEW

In [6-8] introduced three deep learning models that have been based on Deep Recurrent Neural Networks (DRNN) for Fault Region Identification, Fault Type Classification, and Fault Location Prediction; their models utilised methods like Phasor Measurement Units data for processing the input features. By the process of employing a Sequential Deep Learning (SDL) method through the application of Long Short-Term Memory (LSTM), they showed that their models have excelled in modelling spatiotemporal sequences by which they had shown better detection and classification performance in a Two-Area Four-Machine Power System under various fault conditions.

The [9-10] had attempted to propose a hybrid Quantum Computing (QC)-based deep learning framework that was designed to merge the Feature Extraction (FE) capability of the conditional restricted Boltzmann machine with that of the efficient classification ability functions through deep networks. This approach has been designed with a focus on addressing the computational challenges and has experimented with demonstrating the high efficiency and improved fault diagnosis performance together with quick response times on a simulated environment with 30-bus HEPS in which their model had outperformed other traditional ANN and decision tree methods.

Authors [11-12] had been involved in the presentation of a FDM that is employed for switching power supply failure detection. Their method was dubbed DTDBN. Their work involved the isolation and analysis of grid voltage data in order to diagnose the filter capacitor faults. Their method achieved high recognition rates for capacitor states, thereby showcasing the method's effectiveness for classification and early alert of power capacitor faults.

In [13-14] have introduced a Fault Classification Method (FCM) that uses Deep Belief Networks (DBN) for distribution networks. The fault current and voltage samples all undergo the preprocessing steps, after which the data are used to train the DBN. This method employing the automatic FE and efficient fault type classification model has demonstrated high accuracy and better adaptability under various network conditions.

The [15-16] have employed the DL model for the purpose of power system FDM through an improved DBN model that has used a 30-dimensional feature set to map the relationship between grid faults to that of the system features, which are further refined by an extreme ML. Their method has displayed enhanced FE capabilities that have shown better diagnostic accuracy when compared to that of standard AI methods in various failure scenarios.

III. METHODOLOGY

Monitoring Infrastructure

The monitoring infrastructure that had been designed for the proposed CDBN-ES in HEPS is built with the objective of managing the diversity in factors like generator configurations, construction, operating conditions, and orientations, which can be done only through precise instrumentation and data management [17]. This system has particularly incorporated shaft vibration monitoring that is aligned with ISO Standard 13373-74, which involves the strategic placement of non-contacting proximity probes that are essential to measure shaft relative vibration and bearing housing vibration at guide bearings. The infrastructure also employs sensors that are needed to gauge the air gap between the rotor and stator, which can better offer insights about the air gap dimensions, circularity, and concentricity in compliance with CEATI International standards. This setup is further complemented with vibration and dynamic pressure sensors to monitor the forces acting on the runner, including the static and the dynamic pressures. This is done using advanced tools like Bently Nevada's 350300 Dynamic Pressure sensor. The following **Fig 1** shows common sensor measurements and the corresponding malfunctions that can be diagnosed using it.

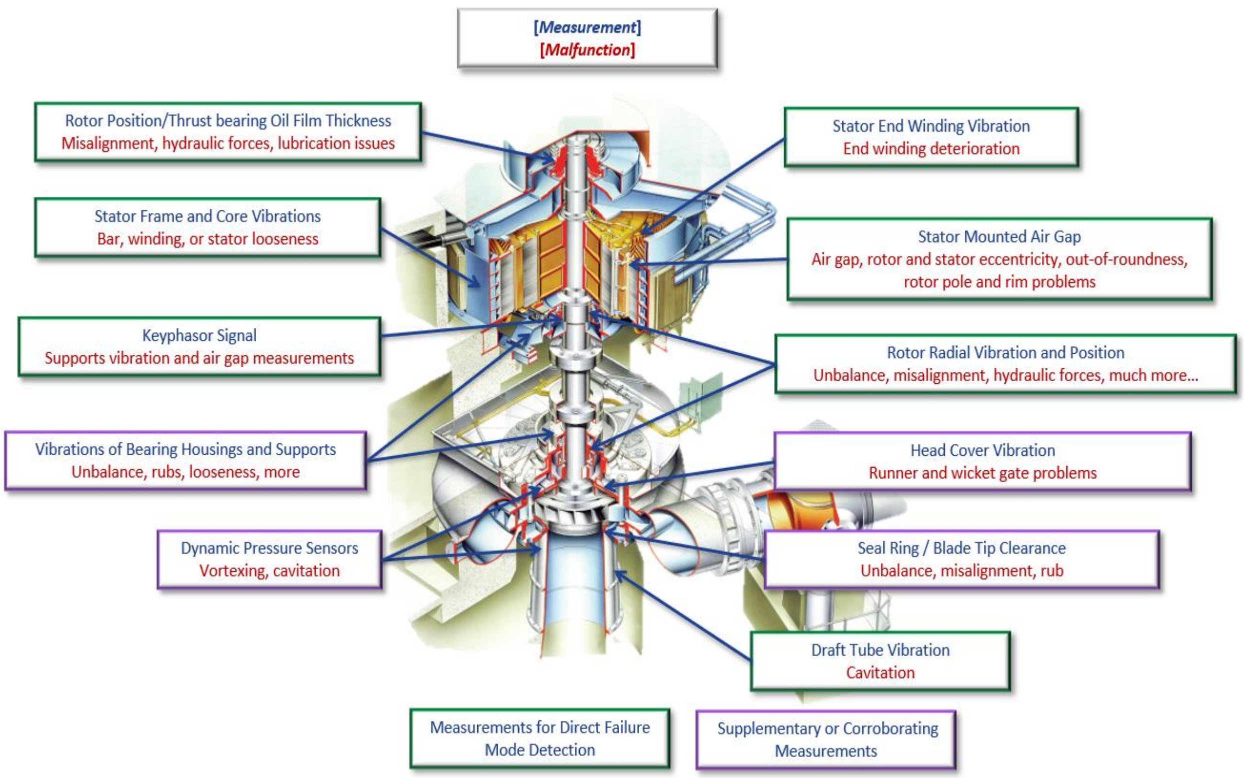

Fig 1. Typical Measurements and Some Corresponding Malfunctions

Data that are collected from the sensors are subjected to preprocessing that filters noise out of the data and normalizes the signals from these sensors to ensure the quality and reliability of data that are further fed into the learning model for analysis. The infrastructure includes manageable, scalable storage systems for the purpose of archiving processed data to facilitate efficient data retrieval for model training and validation. The monitoring infrastructure is integrated into a processing computer to handle the computational demands of analyzing data through the CDBN-RBM model. The expert system built using the learning model is of the purpose to that it handles the stored data in order to Anomaly Detection (AD) and try to diagnose faults. Also, it continuously refines its accuracy by learning from historical data [19-20]. An integrated alert system is also built into this infrastructure, and its purpose is to notify the plant operators if any potential issues are identified. It also categorizes the alerts by severity level to prompt the correct level of appropriate responses.

Fault Detection Model (FDM)

Hydroelectric generators are all very much subjected to various environmental and mechanical stresses, including fluctuating water flow rates, mechanical wear and tear, temperature variations, and the accumulation of sediments or debris. All these conditions have necessitated the need for a robust system that is capable enough of distinguishing between two primary failure modes:

Hard Failures: These are failures that are characterized by sudden and catastrophic malfunctions, which are often triggered by acute stresses such as extreme load conditions or rapid mechanical obstructions. Hard failures are those failures that demand immediate attention to prevent extensive operational disruption and the occurrence of any possible damage to the generator system. The causes of hard failures can be broadly classified into two main types, each requiring a distinct predictive approach by the FDM:

Extreme Load Model: To account for the nonlinear impact of extreme loads, this model uses a power-law relationship, recognizing that failure probability may increase disproportionately with load, EQU (1)

$$P_{\text{extreme}}\,(y = 1 \mid X, L) = \sigma\left(w^T X + \alpha L^{\beta} + b\right) \tag{1}$$

- L represents the load factor, with $L > 1$ indicating extreme load conditions.
- α and β are parameters that capture the nonlinear relationship between load factors and the probability of failure, with β typically greater than 1 to model the accelerated risk under extreme load.
- σ is the sigmoid function, ensuring the output probability remains between 0 and 1.

Rapid Stress Model Given the dynamic nature of rapid stressors, a differential approach highlights the rate of change in operational conditions, EQU (2)

$$P_{\text{rapid}}\,(y = 1 \mid X, S) = \sigma\left(w^T X + \gamma \frac{dS}{dt} + b\right) \tag{2}$$

- S represents a stress indicator,
- $\frac{dS}{dt}$ Quantifies the rate of change in stress.
- γ is a weight parameter for the rate of change in stress.

Soft Failures: In contrast, soft failures are failures that develop gradually and most probably result from the process of continuous operations under normal or mildly stressful conditions. These failures manifest as a progressive decline in performance that, as a result, eventually culminates in a breakdown if it is not addressed promptly. The FDM approaches soft failures through the gradual aging model, and wear, and tear are due to operational stress.

Gradual Aging Model: To capture the effects of aging, we introduce an aging index A, which accumulates over time based on operational history and environmental conditions, EQU (3).

$$P_{\text{aging}}\,(y = 1 \mid X, A) = \frac{1}{1 + e^{-(w^T X + \alpha A + b)}} \tag{3}$$

Here, α is a coefficient that quantifies the impact of aging on the likelihood of a soft failure, and A is the aging index calculated from operational and environmental data.

Wear and Tear due to Operational Stress: The cumulative operational stress experienced over time as S, which contributes to wear and tear. The amount of wear and tear accumulated can be modelled using the Gamma distribution, characterized by shape (α) and scale (θ) parameters, EQU (4).

$$P(S; \alpha, \theta) = \frac{1}{\Gamma(\alpha)\theta^{\alpha}} S^{\alpha - 1} e^{-\frac{S}{\theta}} \tag{4}$$

- S represents the cumulative operational stress.
- $\alpha > 0$ is the shape parameter.
- $\theta > 0$ is the scale parameter.

In this context, $P(S; \alpha, \theta)$ estimates the probability density function of the wear and tear accumulation due to operational stress S, allowing for the prediction of maintenance needs based on the observed stress patterns.

Leveraging the sensor data from the critical generator components, the designed FDM analyzes the measurements corresponding to the vibration, temperature, and load metrics. Using these measurements, the prediction model can simulate the generator's condition accurately and predict possible impending failures.

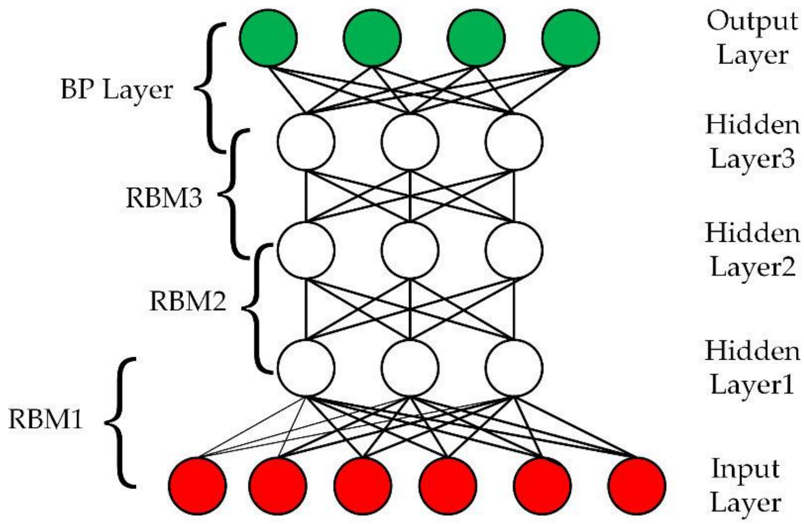

Fig 2. DBN-RBM Architecture

Deep Belief Network-Restricted Boltzmann Machine (DBN-RBM)

DBNs are a class of DNNs that consist of multiple layers of stochastic, latent variables (**Fig 2)**. The top two layers form an associative memory, and the lower layers form a belief network with directed, generative connections. The building blocks of DBN are RBM, which are undirected graphical models that learn to reconstruct the input data by finding the best possible representation in the latent space.

An RBM consists of visible units v (representing input data) and hidden units h (representing features or patterns learned from the data), with bidirectional, symmetric connections between them. There are no connections between units of the same layer, making the structure "restricted." The energy of a joint configuration (v, h) in the RBM is defined as:

$$E(v,h) = -\sum_i a_i v_i - \sum_j b_j h_j - \sum_{i,j} v_i h_j w_{ij} \tag{5}$$

where a_i and b_j are biases for visible unit i and hidden unit j, respectively, and w_{ij} is the weight between visible unit i and hidden unit j. The probability of a configuration is given by the Boltzmann distribution:

$$P(v,h) = \frac{1}{Z} e^{-E(v,h)} \tag{6}$$

where Z is the partition function, a normalizing constant obtained by summing over all possible pairs of v and h. The updated rules for the weights and biases are derived from this approximation:

$$\Delta w_{ij} = \epsilon\left(\langle v_i h_j\rangle_{\text{data}} - \langle v_i h_j\rangle_{\text{recon}}\right) \tag{7}$$

$$\Delta a_i = \epsilon(\langle v_i\rangle_{\text{data}} - \langle v_i\rangle_{\text{recon}}) \tag{8}$$

$$\Delta b_j = \epsilon\left(\langle h_j\rangle_{\text{data}} - \langle h_j\rangle_{\text{recon}}\right) \tag{9}$$

where ϵ is the learning rate. A DBN is formed by stacking multiple RBMs, where the hidden layer of one RBM serves as the visible layer for the next.

In the context of employing the DBN model in fault diagnosis, the DBN is trained to learn a hierarchical representation of the standard operational data of the power system. Once trained, the DBN is applied to AD or faults by evaluating how well new data fits the learned model. Anomalies are detected when the reconstruction error exceeds a predetermined threshold, indicating that the model encounters patterns that significantly deviate from the norm, suggesting potential faults.

Convolutional Deep Belief Network (CDBN) Model

The CDBN model adapts the CNN architecture, featuring weight sharing across its hidden and visible layers, which is effectively applied to each position within the data matrix. This model's architecture is illustrated as follows:

The CDBN architecture (**Fig 3)** comprises three principal layers: a visible input layer V, a hidden layer H, and a pooling layer P. The input layer V is represented as a binary matrix of dimensions $N_V \times N_V$. Assuming the presence of K convolutional kernels, each dimension $N_W \times N_W$, the hidden layer then generates K-dimensional feature maps of size $N_H \times N_H$ (where $N_H = N_V - N_W + 1$). The hidden layer's output undergoes dimensionality reduction via the pooling layer to yield an output of size $N_P \times N_P$. Each feature point P^k within the pooling layer correlates to a specific $C \times C$ area α in the hidden layer, with B_α denoting the set of indices corresponding to area α.

Activation and Reconstruction

The hidden layer's activation probability and the input layer's reconstruction probability are described by the following expressions: EQU (10 and EQU (11).

- For hidden layer activation:

$$P\left(h_{ij}^k = 1 \mid V, \theta\right) = \sigma\left(\left(\tilde{W}^k * V\right)_{ij} + b_k\right) \tag{10}$$

- For input layer reconstruction:

$$P\left(V_{ij}^k = 1 \mid h, \theta\right) = \sigma\left(\left(\sum_k W^k * h^k\right)_{ij} + a\right) \tag{11}$$

Here, $\sigma(x) = \frac{1}{1+e^{-x}}$ denotes the sigmoid activation function, $\tilde{W}^k = W^k_{(N_W - j+1)}$, and '*' represents the convolution operation. The parameters include a, the bias for the visible layer, and $b = \left(b_1, b_2, \ldots, b_{n_h}\right)^T$, the bias vector for the hidden layer, with $\theta = (W, a, b)$ encapsulating the model's parameters.

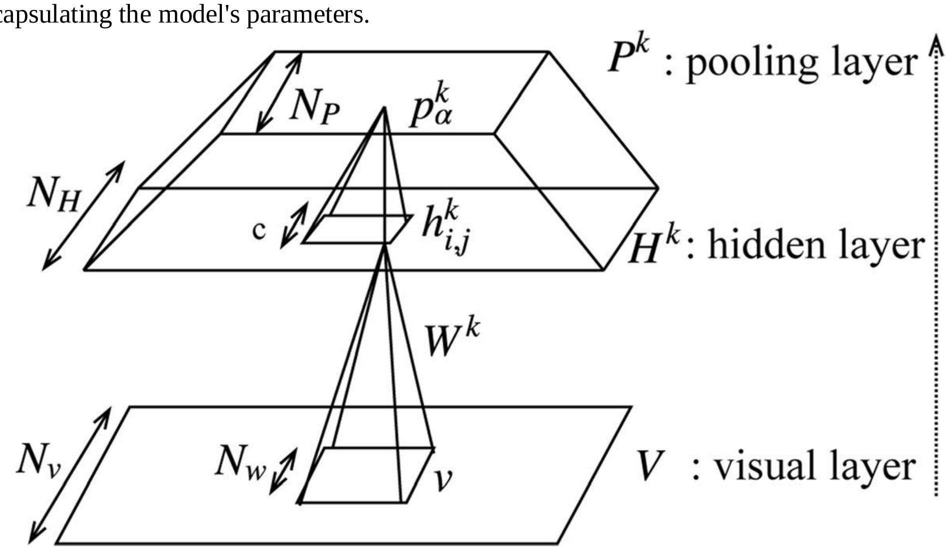

Fig 3. Convolutional Deep Belief Network (CDBN) Model

Pooling Layer Activation: The activation probability for each feature point in the pooling layer is derived from the maximum probability across the corresponding $C \times C$ region within the hidden layer. This conditional probability, based on maximum probability pooling, is defined as EQU (12).

$$P\left(h_{ij}^k = 1 \mid V, \theta\right) = \frac{e^{I\left(h_{ij}^k\right)}}{1+\sum_{(m,n)} e^{I\left(h_{mn}^k\right)}} \tag{12}$$

where $I\left(h_{ij}^k\right) = \left(\tilde{W}^k * V\right)_{ij} + b_k$ signifies the net activation for the k-th channel in the hidden layer, facilitating the following pooling probability, EQU (13)

$$P(p_\alpha^k = 0 \mid V, \theta) = \frac{1}{1+\sum_{(i,j)\in B_\alpha} e^{I\left(h_{ij}^k\right)}} \tag{13}$$

Algorithm for *CDBN-Based Fault Detection System*

Phase 1: Training

Input: Training dataset $T = \{(x_1, y_1), (x_2, y_2), \dots, (x_n, y_n)\}$, where x_i is the ith sensor data instance, and y_i is its label (normal, soft failure, hard failure).

Parameters: Number of layers L, convolutional kernel sizes $\{K_1, K_2, \dots, K_L\}$, learning rate η, pooling window size $C = 2$.

1. $T = \text{Normalize}(T)$
2. Initialize CDBN with L layers, each with a specified kernel size K_i, random weights W_i, and biases b_i.
3. FOR EACH layer l from 1 to L Do:
   3.1. Input_Layer = $(l == 1)$? T : Output of $(l-1)$-th layer
   3.2. Apply Convolution with Sigmoid Activation:
   $$ConvOutput = Sigmoid(Convolve(InputLayer, K_i, W_i))$$
   3.3. Apply Max Pooling: $PoolOutput = MaxPool(ConvOutput, C)$
   3.4. Train RBM on pooled output (Contrastive Divergence): $[W_i, b_i] = TrainRBM(PoolOutput, W_i, b_i, \eta)$
4. Fine-tune the entire network using backpropagation with learning rate η.
5. Evaluate the model on a validation set and adjust parameters as needed.

Phase 2: Fault Detection (Prediction)

Input: New sensor data instance N.

Output: Fault diagnosis class (normal, soft, hard failure).

1 $N = \text{Normalize}(N)$
2 FE $= N$
3 For Each layer l from 1 to L, do:
  3.1 Apply learned transformations:
  $ConvOutput = Sigmoid(Convolve(FE, K_i, W_i))$
  3.2 $PoolOutput = MaxPool(ConvOutput, C)$
  3.3. FE = $PoolOutput$
4 $Diagnosis = Softmax(Classify(FE))$// Classify using softmax
5 Return Diagnosis

IV. EXPERIMENT ANALYSIS

This section presents the details about applying the CDBN model on data from Huóshuǐ Small Hydropower, which includes 88 hydropower plants with capacities from 0.1 to 14 MW. The experimental study used data sourced from two generators, GR04 and GR17, over a 12-month period from April 2022 to March 2023. The Data were recorded every 15 minutes and covered the operational parameters such as temperature, vibration, flow rates, and pressure. The energy output of these plants during the observed period is shown in **Fig 4**, and the count of the detected failures during this experiment period of time is outlined in **Table 1** and depicted in **Fig 5.**

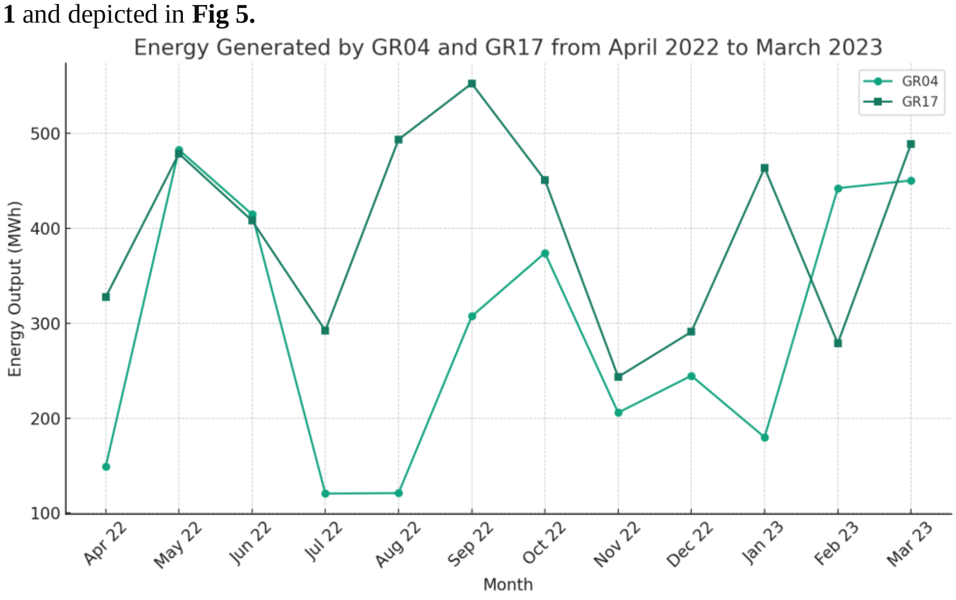

Fig 4. Energy Output for the Studied Period

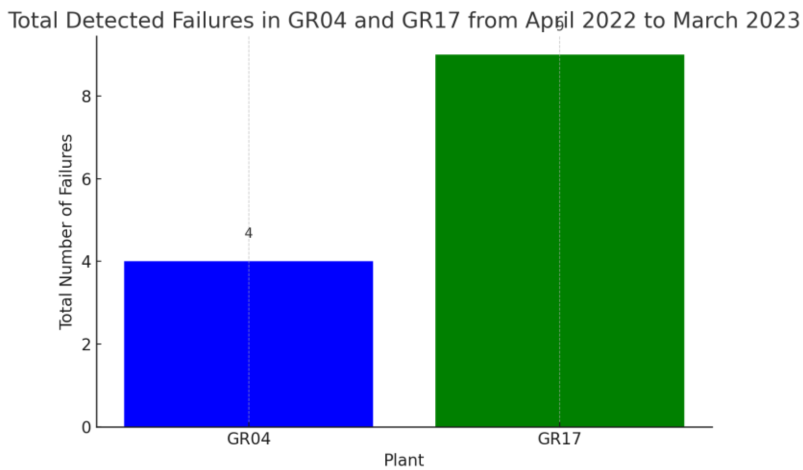

Fig 5. Detected Failures for the Studied Period

Table 1. Detailed Description of FDM

Generator ID	Component	Timestamp	Observations
GR04	Gearbox	2022-06-15 08:30	Excessive vibration detected
GR04	Transformer	2022-08-22 14:00	Temperature anomaly detected
GR04	Bearings	2022-10-09 11:45	Increased noise level observed
GR04	Rotor	2022-12-19 13:20	Rotor misalignment identified
GR17	Generator	2022-07-05 09:45	Irregular power output observed
GR17	Bearings	2022-08-21 10:15	Bearing wear detected
GR17	Stator	2022-10-30 12:00	Stator insulation failure
GR17	Control System	2022-11-15 14:30	Control system malfunction
GR17	Turbine	2023-01-10 09:00	Turbine blade erosion
GR17	Sensor	2023-02-25 10:20	Sensor malfunction
GR17	Cooling System	2023-03-05 08:15	Cooling system inefficiency
GR17	Valve	2023-03-20 09:35	Valve leakage
GR17	Electrical Wiring	2023-03-31 11:50	Electrical wiring corrosion

The sensor data that were collected from both generators during the experiment amounted to a total of 3,348,791 data samples with a missing rate of 0.24%. This dataset comprised 34 attributes that were fed into the FDM. The FDM derived at the following values as shown in **Table 2**.

Table 2. Parameters and Values in the FDM

Parameter	Description	l Value
L	Load Factor, indicating extreme load conditions	>1
α	Parameter capturing the nonlinear relationship between load and failure probability for hard failures	2.5
β	Parameter indicating the risk acceleration under extreme load for hard failures	1.5
γ	Weight parameter for the rate of change in stress, emphasizing rapid variations for rapid stress model	0.075
A	Aging index, accumulating over time based on operational history and environmental conditions for gradual aging	3500
S	Cumulative operational stress experienced, contributing to wear and tear	Varies
α (Gamma distribution)	Shape parameter for the gradual aging model, related to the frequency of stress events	9.0
β (Gamma distribution)	Scale parameter for the gradual aging model, related to the severity of each stress event	2500
δ	The critical interval for stress accumulation in the rapid stress model	0.1
τ	Time until likely failure under specific stress conditions	4 hours
λ	Rate of stress events per unit time (Poisson process) for operational stress	0.03 events/hour

After performing the configuration of the failure parameters, the FDM is executed iteratively 50 times to record ten failures precisely. This iteration has resulted in a dataset with 354,621 samples. 80% is used for training, and the remaining 20% is used for testing. The designed CDBN is trained using the following parameters as shown in **Table 3**.

Table 3. CDBN Hyperparameters for FDM

Hyperparameter	Hypothetical Value
Number of Layers	5
Convolutional Kernel Size	3x3
Pooling Size	2x2
Feature Maps	128
Learning Rate	0.01
Momentum	0.9
Weight Decay	0.0005
RBM Learning Rate	0.005
RBM Training Epochs	100
Fine-tuning Epochs	50
Batch Size	64
Activation Function	ReLU (for convolutional layers), Sigmoid (for RBM layers)

Deviation Measurement

The control chart used for deviation measurement employed the statistical measures that had defined control limits to analyse the expected range of deviations and find the discrepancies showing model prediction errors or shifts in system behaviour. The central line (CL) in a control chart represents the mean value of the measured deviations, calculated as $CL = \frac{1}{n}\sum_{i=1}^{n}(y_i - \hat{y}_i)$, where y_i is the actual value, $\hat{y}_i$ is the predicted value by the FDM, and n is the number of observations. Upper Control Limit (UCL) and Lower Control Limit (LCL) are set based on standard deviations from the mean, typically at $\pm 3\sigma$, where σ is the standard deviation of the deviations. The following **Fig 6, Fig 7 and Fig 8** show the deviations measured for stress value, vibration frequency and temperature compared for both generators.

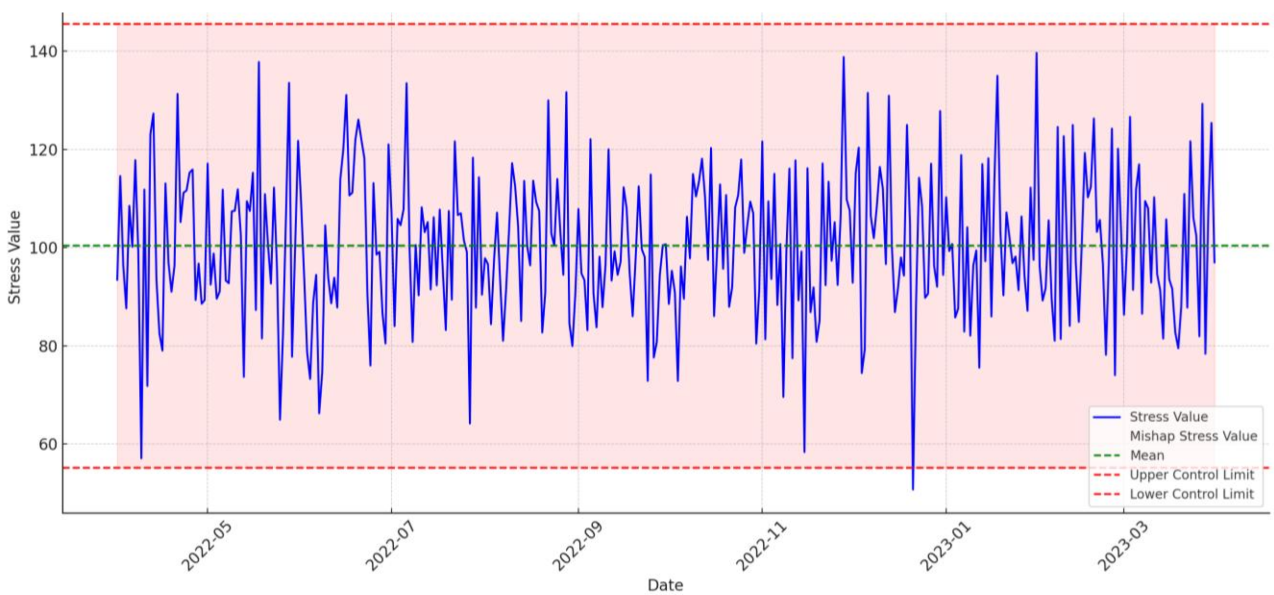

(a) GR04

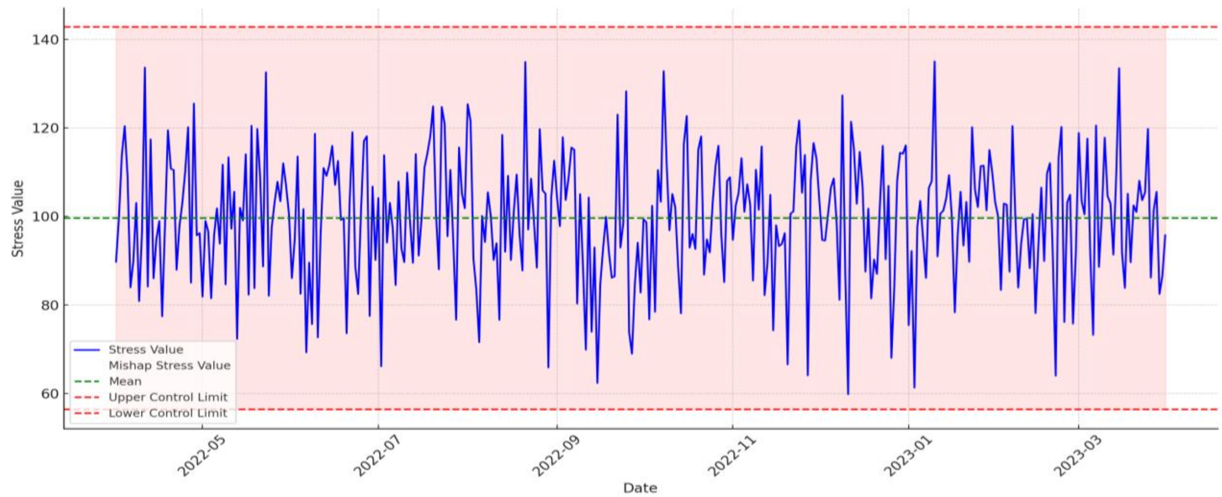

(b) GR17

Fig 6. Stress value assessment for (a) GR04 and (b) GR17

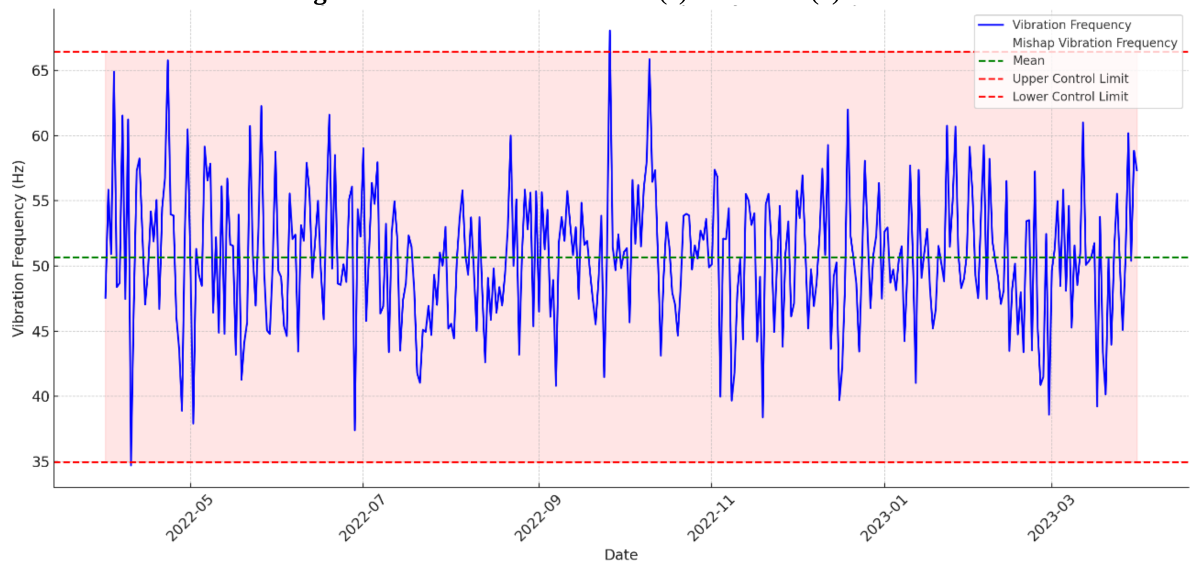

(a) GR04

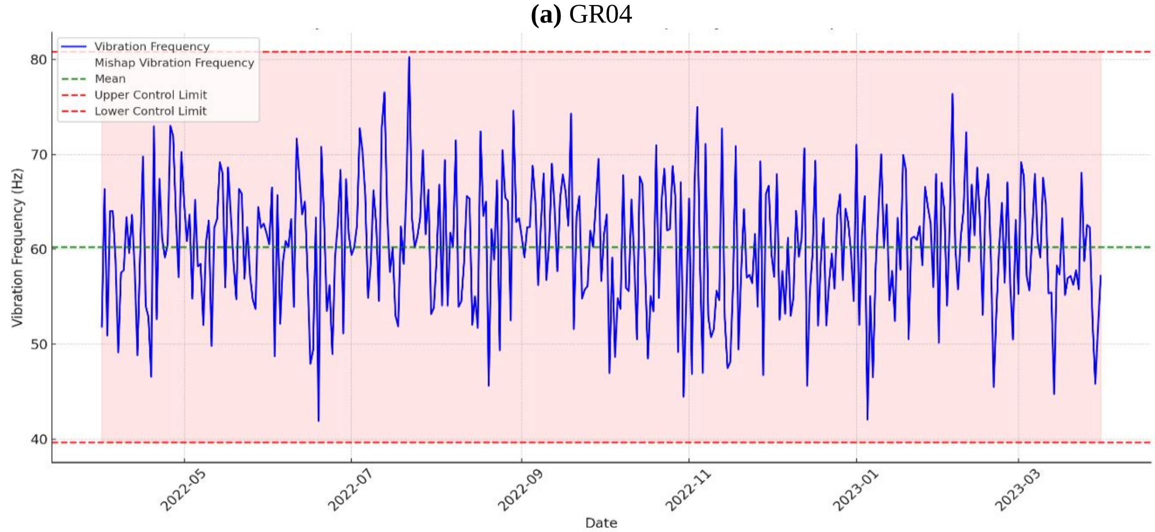

(b) GR17

Fig 7. Vibration Frequency assessment for (a) GR04 and (b) GR17

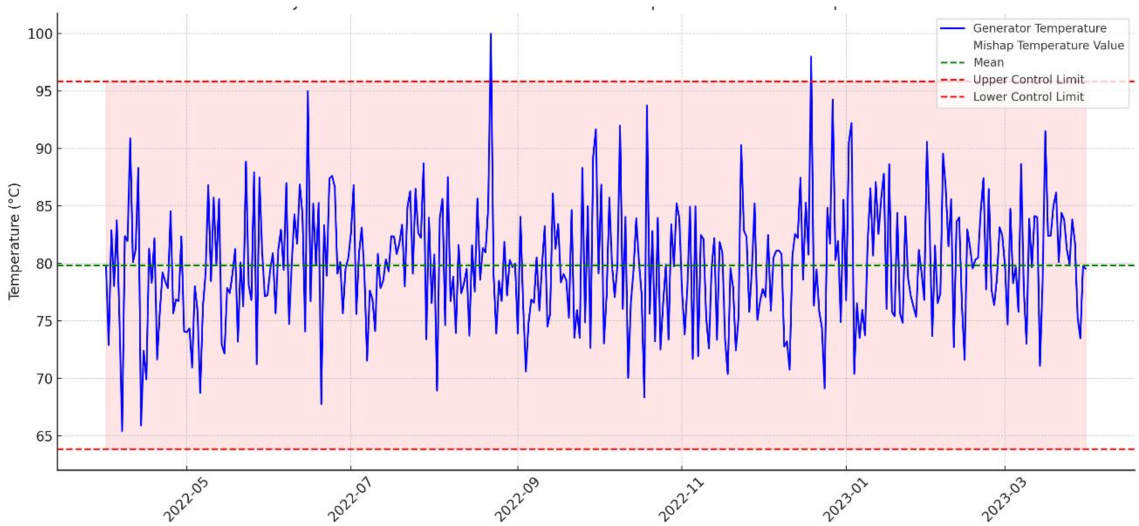

(a) GR04

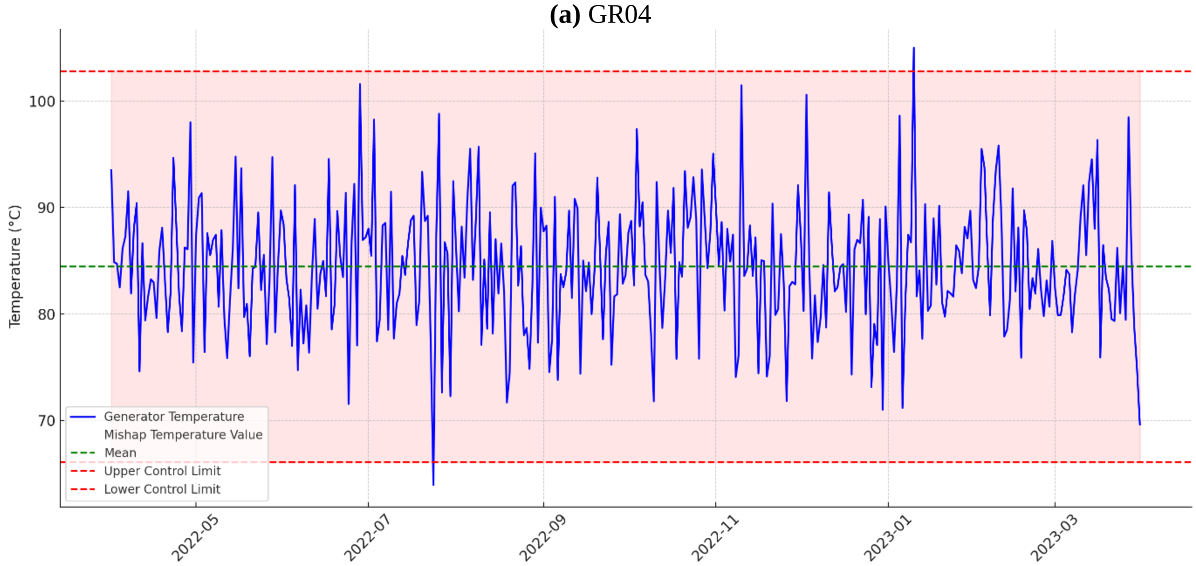

(b) GR17

Fig 8. Temperature assessment for (a) GR04 and (b) GR17

The trained CDBN model was compared against i) DBN, ii) CNN, iii) LSTM using the following metrics such as:

Accuracy: Accuracy measures the overall correctness of the model across all classes. It is calculated as the ratio of correct predictions (TP and TN) to the total number of cases, EQU (14)

$$\text{Accuracy} = \frac{TP+TN}{TP+TN+FP+FN} \tag{14}$$

Where:

- TP = True Positives: The count of TP correctly predicted by the model.
- TN = True Negatives: The count of TN correctly predicted by the model.
- FP = False Positives: The count of TN incorrectly predicted as positives.
- FN = False Negatives: The count of TP incorrectly predicted as negatives.

Precision (Positive Predictive Value): Precision assesses the model's ability to correctly predict positive (failure) instances among all instances predicted as positive. It's crucial when the cost of FP is high, EQU (15).

$$\text{Precision } = \frac{TP}{TP+FP} \tag{15}$$

Recall (Sensitivity or True Positive Rate (TPR)): Recall evaluates the model's capability to identify all TP cases. It is critical when the cost of missing a positive (failure) case is significant, EQU (16)

$$\text{Recall} = \frac{TP}{TP+FN} \tag{16}$$

F1-Score: The F1-score provides a balance between Precision and Recall, useful when there's an uneven class distribution or when FP and FN have different implications, EQU (17).

$$\text{F1-Score } = 2 \times \frac{\text{Precision} \times \text{Recall}}{\text{Precision} + \text{Recall}} \tag{17}$$

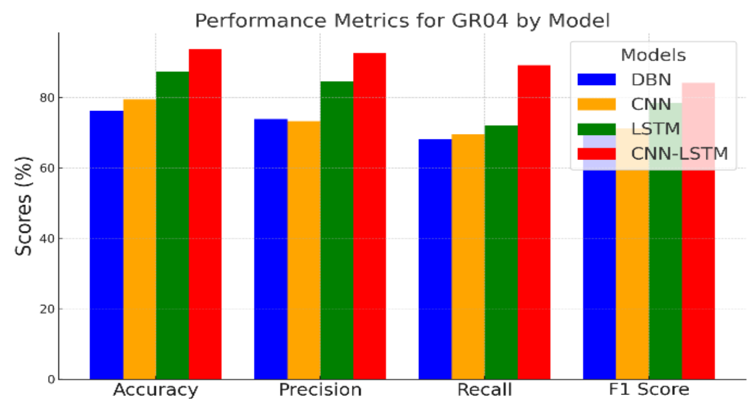

Fig 9. Performance comparison for GR04

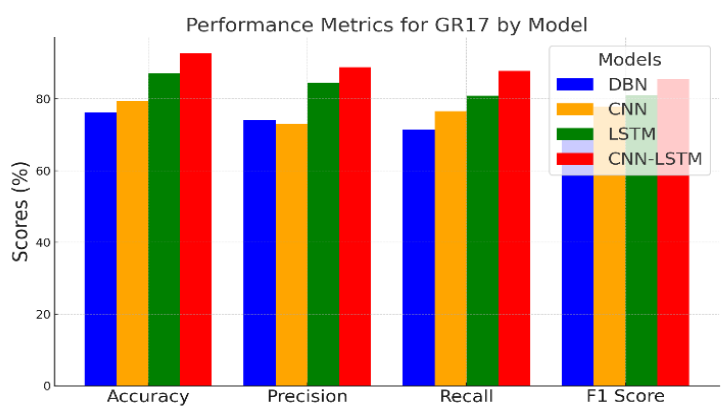

Fig 10. Performance comparison for GR17

The performance analysis of FDM in GR04 and GR17, as shown in **Fig 9** and **Fig 10**, reveals distinct outcomes. For GR04, the DBN model shows lower performance with accuracy at 76.23%, precision at 73.89%, recall at 68.06%, and an F1-score of 70.36%. The CNN model slightly improves accuracy to 79.46% but offers similar precision and a modest increase in recall and F1-score. The LSTM model marks a significant leap, especially in recall (72.02%) and F1-score (78.42%), indicating its better capability in identifying TP. The CNN-LSTM model tops the charts with the highest accuracy (93.74%), precision (92.66%), recall (89.17%), and F1-score (84.16%), showcasing its comprehensive feature learning.

For GR17, the DBN model replicates its performance from GR04, indicating similar limitations. The CNN model shows a slight decrement in accuracy to 79.31% but improves recall and F1-score, suggesting slightly better identification of TP compared to GR04. The LSTM model again significantly improves, particularly in recall (80.84%) and F1-score (81.08%), underscoring its effectiveness in sequential data analysis. The CNN-LSTM model remains the best performer with accuracy at 92.59%, precision at 88.86%, recall at 87.74%, and F1 score at 85.6%, albeit with slightly different margins of improvement over LSTM compared to GR04.

V. CONCLUSION AND FUTURE WORK

A Convolutional Deep Belief Network-based Expert System (CDBN-ES) for autonomous fault diagnosis in Hydro-Electrical Power Systems (HEPS) has been created and implemented as the outcome of the findings from this study. By evaluating the outcomes of the Convolutional Deep Belief Network (CDBN) against that of different Deep Learning (DL) models like DBN, CNN, and LSTM, the researchers discovered that CDBN has done superior in detecting and classifying both hard and soft failures in hydro-electric generators. The data that was used for the assessment originated from the GR04 and GR17 generators. Key performance metrics, namely accuracy, precision, recall, and F1-score, were improved by the CDBN approach. Conventional FDM has its errors, as the researchers highlighted; for instance, numerous models depend on reactive methods, which may not be robust enough to deal with the complex dynamics of HEPS failures.

Boosting the framework's predictive accuracy will be the most important objective of future research. This will be feasible by additional model optimisation. Furthermore, it is going to examine possible factors in the environment and data sources that might possess significant consequences on how well the system performs.

Data Availability
No data was used to support this study.

Conflicts of Interests
The author(s) declare(s) that they have no conflicts of interest.

Funding
No funding agency is associated with this research.

Competing Interests
There are no competing interests.

References
[1]. P. M. Musyoka, “Development of Optimized Under-Frequency Load-Shedding Scheme With Renewable-Energy Integration,” (Doctoral dissertation, University of Nairobi), 2020.
[2]. F. Calabrese, A. Regattieri, M. Bortolini, F. G. Galizia, and L. Visentini, “Feature-Based Multi-Class Classification and Novelty Detection for Fault Diagnosis of Industrial Machinery,” Applied Sciences, vol. 11, no. 20, p. 9580, Oct. 2021, doi: 10.3390/app11209580.
[3]. C. Y. Kang, “Design of Hydro Turbine Management Unit for Standalone Pico Hydro in Rural Area (Doctoral dissertation,” Swinburne University of Technology Sarawak Campus), 2023.
[4]. J. Penfield and M. Holland, “Machine Learning Based Online Monitoring of Step-Up Transformer Assets in Electrical Generating Stations,” 2021 9th International Conference on Smart Grid (icSmartGrid), Jun. 2021, doi: 10.1109/icsmartgrid52357.2021.9551264.
[5]. S. Akhtar, M. Adeel, M. Iqbal, A. Namoun, A. Tufail, and K.-H. Kim, “Deep learning methods utilization in electric power systems,” Energy Reports, vol. 10, pp. 2138–2151, Nov. 2023, doi: 10.1016/j.egyr.2023.09.028.
[6]. S. Belagoune, N. Bali, A. Bakdi, B. Baadji, and K. Atif, “Deep learning through LSTM classification and regression for transmission line fault detection, diagnosis and location in large-scale multi-machine power systems,” Measurement, vol. 177, p. 109330, Jun. 2021, doi: 10.1016/j.measurement.2021.109330.
[7]. Y. Zhang, Y. Zhang, L. Wen, Z. Cui, Y. He, and G. Liu, “Power Grid Fault Diagnosis Based on Improved Deep Belief Network,” Journal of Physics: Conference Series, vol. 1585, no. 1, p. 012021, Jul. 2020, doi: 10.1088/1742-6596/1585/1/012021.
[8]. Z. Chen et al., “Thermal Fault Diagnosis of Power Equipment through Improved Instance Segmentation Algorithm and Deep Neural Network Temperature Fitting,” 2023 3rd International Conference on New Energy and Power Engineering (ICNEPE), Nov. 2023, doi: 10.1109/icnepe60694.2023.10429092.
[9]. K. Li, B. Zhao, M. Liu, X. Wang, G. Zhang, and M. Sun, “Automated Diagnosis of Lightning Faults on Transmission Lines,” 2020 IEEE 5th Information Technology and Mechatronics Engineering Conference (ITOEC), Jun. 2020, doi: 10.1109/itoec49072.2020.9141606.
[10]. Y. Cai and M. -Y. Chow, "Small world stratification for distribution fault diagnosis," IEEE/PES Power Systems Conference and Exposition, Phoenix, AZ, USA, 2011, pp. 1-6, doi: 10.1109/PSCE.2011.5772508.
[11]. N. Zhou, W. Li, and J. Zhou, “Fault Diagnosis for Tray Loader Machine of Power Battery Based on Fault Tree Analysis,” 2018 IEEE 3rd Advanced Information Technology, Electronic and Automation Control Conference (IAEAC), Oct. 2018, doi: 10.1109/iaeac.2018.8577788.
[12]. B. Sun, F. Wang, F. Shi, H. Zhang, C. Fang, and S. Liu, “Development and Automated Testing Platform for Active Distribution Network Fault Diagnosis Module,” 2019 IEEE 2nd International Conference on Electronics Technology (ICET), May 2019, doi: 10.1109/eltech.2019.8839397.
[13]. C. Diendorfer et al., “Graph traversal-based automation of fault detection, location, and recovery on MVDC shipboard power systems,” 2017 IEEE Second International Conference on DC Microgrids (ICDCM), Jun. 2017, doi: 10.1109/icdcm.2017.8001032.
[14]. S. Dheepadharshani, S. Anandh, K. B. Bhavinaya, and R. Lavanya, “Multivariate Time-series Classification for Automated Fault Detection in Satellite Power Systems,” 2019 International Conference on Communication and Signal Processing (ICCSP), Apr. 2019, doi: 10.1109/iccsp.2019.8698017.
[15]. M. Kinnaert and L. Rakoto, “Model-based fault diagnosis for wind turbines? Can it work in practice?” 2016 3rd Conference on Control and Fault-Tolerant Systems (SysTol), Sep. 2016, doi: 10.1109/systol.2016.7739835.
[16]. B. Ilhem, B. Amar, A. Lebaroud, and R. Fares, “Automatic fault diagnosis of fault tolerant power converter for switched reluctance motor based on time-frequency technique,” 2014 16th International Power Electronics and Motion Control Conference and Exposition, Sep. 2014, doi: 10.1109/epepemc.2014.6980680.